TiS Trends in Sciences
TRENDS IN SCIENCES 2027; 24(1): 14177
SPRINT Scholarly Publishing and Repository Integration Center
https://doi.org/10.48048/tis.2027.14177
RESEARCH ARTICLE

Paclitaxel-Conditioned Mesenchymal Stem Cells Enhance T Cell Activation and Cytotoxicity Against CD44^{+}/CD24^{-} Breast Cancer Stem Cells

Dedy Hermansyah[1,*], Siti Syarifah[2], Adi Muradi Muhar[3] and Nur Dina Amalina[4,5,6]

[1]Department of Surgery, Faculty of Medicine, Universitas Sumatera Utara, North Sumatera, Medan, Indonesia
[2]Department of Pharmacology, Faculty of Medicine, Universitas Sumatera Utara, North Sumatera, Medan, Indonesia
[3]Department of Doctoral Degree Program, Faculty of Medicine, Universitas Sumatera Utara, North Sumatera, Medan, Indonesia
[4]Pharmaceutical Sciences Department, Faculty of Medicine, Universitas Negeri Semarang, Semarang, Indonesia
[5]Stem Cell and Cancer Research Indonesia, Semarang, Indonesia
[6]Biotechnology Study Program, Agung Putra University, Semarang, Indonesia

([*]Corresponding author's e-mail: dedi.hermasyah@usu.ac.id)

Received: 23 April 2026, Revised: 11 June 2026, Accepted: 21 June 2026, Published: 25 August 2026

Abstract

Breast cancer stem cells (BCSCs) represent a critical population responsible for tumor recurrence, metastasis, and therapeutic resistance. Despite advances in immunotherapy, targeting BCSCs remains challenging due to their immune evasion mechanisms and limited T cell infiltration. To investigate the potential of paclitaxel-conditioned mesenchymal stem cells (MSCs) in enhancing T cell activation and cytotoxicity against CD44^{+}/CD24^{-} breast cancer stem cells. BCSCs were isolated from MDA-MB-231 cells using magnetic-activated cell sorting (MACS) and characterized by flow cytometry. MSCs derived from umbilical cord blood were treated with paclitaxel (10 - 20 µg/mL) for 72 h to generate conditioned medium (CM-MSCs-Pax). CD8+ T cells were isolated from tumor-bearing BALB/c mice and activated using CM-MSCs-Pax. T cell activation was assessed by IL2RA (CD25) expression via qRT-PCR. Co-culture experiments evaluated cytotoxicity against BCSCs using the MTT assay, and molecular mechanisms were examined by analyzing caspase-3 and PD-L1 expression. MACS sorting successfully enriched CD44^{+}/CD24^{-} BCSCs to 80.7% purity. Paclitaxel treatment significantly enhanced MSC secretion of IL-6, TNF-α, and IL-10 in conditioned medium. CM-MSCs-Pax treatment increased T cell activation, demonstrated by elevated IL2RA expression. Co-culture of activated T cells with BCSCs at a 10:1 ratio reduced BCSC viability to 9.68% at 72 h compared to 30.20% with unactivated T cells. This enhanced cytotoxicity was associated with increased caspase-3 expression and reduced PD-L1 expression in BCSCs. Paclitaxel-conditioned MSCs create a pro-inflammatory microenvironment that enhances T cell activation and cytotoxicity against BCSCs. This novel approach combining chemotherapy conditioning with immunotherapy represents a promising strategy for targeting therapy-resistant breast cancer stem cell populations.

Keywords: Breast cancer stem cells, Mesenchymal stem cells, Paclitaxel, T cell activation, Immunotherapy, CD44^{+}/CD24^{-}

Introduction

Breast cancer remains one of the leading causes of cancer-related mortality worldwide, with approximately 2.3 million new cases diagnosed annually [1]. Despite significant advances in therapeutic approaches, tumor recurrence and metastasis continue to pose major clinical challenges. Accumulating evidence suggests that a small population of cells within tumors, termed cancer stem cells (CSCs), plays a pivotal role in driving these processes [2,3]. Breast cancer stem cells (BCSCs) are characterized by self-renewal, multilineage differentiation potential, and resistance to conventional therapies [4,5]. The CD44^{+}/CD24^{-} phenotype has been widely recognized as a reliable marker for identifying

BCSCs in various breast cancer subtypes [6]. These cells exhibit enhanced invasive and metastatic capabilities, contributing to poor clinical outcomes and therapeutic resistance [7,8]. Moreover, BCSCs demonstrate remarkable ability to evade immune surveillance through multiple mechanisms, including upregulation of immune checkpoint molecules such as PD-L1 [9,10].

The tumor microenvironment plays a crucial role in maintaining BCSC stemness and immune evasion properties [11,12]. Mesenchymal stem cells (MSCs) are multipotent stromal cells that naturally home to tumor sites and can significantly influence the local microenvironment [13]. While MSCs have shown promise in cancer therapy due to their tumor-homing properties and immunomodulatory capabilities, their role in cancer remains controversial, with evidence supporting both pro-tumorigenic and anti-tumorigenic effects [13,14]. Recent studies have explored the potential of "educating" or conditioning MSCs to enhance their anti-cancer properties [15]. Paclitaxel, a widely used chemotherapeutic agent that targets microtubules, has been shown to induce immunogenic cell death and promote anti-tumor immune responses [6,16]. We hypothesized that conditioning MSCs with paclitaxel could alter their secretome, creating a pro-inflammatory microenvironment that enhances T cell activation and cytotoxicity against BCSCs. In addition, our previous study showed that paclitaxel-conditioned MSCs exerted direct anti-tumor effects on $CD44^+/CD24^-$ BCSCs by modulating Nrf2 signaling and inducing apoptosis [6]. In contrast, the present study investigates a distinct mechanism in which paclitaxel-conditioned MSCs reshape the cytokine milieu and enhance T cell activation, leading to immune-mediated cytotoxicity against BCSCs. Thus, although both studies examine paclitaxel-conditioned MSCs, the current work extends our earlier findings by shifting the focus from direct tumor cell apoptosis to immune effector cell activation and T cell-dependent killing.

T cell-based immunotherapy has emerged as a promising approach for cancer treatment, particularly through adoptive cell transfer and CAR-T cell technologies [17,18]. However, the efficacy of T cell therapy against solid tumors, particularly BCSCs, remains limited due to the immunosuppressive tumor microenvironment and inadequate T cell activation [19,20]. Enhancing T cell activation through conditioned medium from engineered MSCs represents a novel approach that could overcome these limitations. In this study, we investigated the potential of paclitaxel-conditioned MSCs to enhance T cell activation and cytotoxicity against $CD44^+/CD24^-$ BCSCs. Our findings demonstrate that paclitaxel conditioning significantly alters the MSC secretome, thereby enhancing T cell activation and improving cytotoxicity against therapy-resistant breast cancer stem cells.

Materials and methods

Cell culture and maintenance

MDA-MB-231 human breast cancer cells were cultured in Dulbecco's Modified Eagle's Medium (DMEM) supplemented with 10% fetal bovine serum (FBS) and 1% penicillin-streptomycin at 37 °C in a humidified atmosphere containing 5% CO_2. Human mesenchymal stem cells (MSCs) were isolated from umbilical cord blood following established protocols and cultured in α-MEM supplemented with 10% FBS [21].

Isolation and characterization of breast cancer stem cells

BCSCs were isolated from the human triple-negative breast cancer cell line MDA-MB-231 based on the $CD44^+/CD24^-$ phenotype using magnetic-activated cell sorting (MACS). Cells were cultured under standard conditions until reaching approximately 70% - 80% confluence, then harvested using trypsin-EDTA, neutralized, and washed twice with cold phosphate-buffered saline (PBS) supplemented with 0.5% bovine serum albumin (BSA) and 2 mM EDTA (MACS buffer). For magnetic labeling, cells were first incubated with anti-CD24 microbeads (Miltenyi Biotec) for 15 - 20 min at 4 °C according to the manufacturer's instructions. After washing, the cell suspension was applied to a MACS LS column placed in a magnetic field. The $CD24^+$ cells were retained in the column, while the unlabeled $CD24^-$ fraction was collected in the flow-through. The $CD24^-$ fraction was subsequently incubated with anti-CD44 microbeads for 15 - 20 min at 4 °C. After washing, cells were passed through a new magnetic column, and $CD44^+$ cells were retained and then eluted after removal of the column from the magnetic field, yielding a $CD44^+/CD24^-$ enriched

population. To assess the purity and enrichment efficiency of isolated BCSCs, flow cytometry analysis was performed. Cells were stained with fluorophore-conjugated anti-CD44 and anti-CD24 antibodies (CD44-FITC and CD24-PE; BD Biosciences) and analyzed using a BD FACSCalibur cytometer. Data were processed using FlowJo software to confirm the proportion of $CD44^+/CD24^-$ cells in the sorted population [22].

MSC isolation and culture

Mesenchymal stem cells were isolated from umbilical cord blood samples obtained with informed consent, in accordance with institutional ethical guidelines (Ethics Committee approval number: 074/EC/KEPK/FKUA/2025). Mononuclear cells were separated using Ficoll-Paque density gradient centrifugation (GE Healthcare, Chicago, IL, USA) and plated in tissue culture flasks with Dulbecco's Modified Eagle Medium (DMEM, Gibco, Waltham, MA, USA) supplemented with 10% fetal bovine serum (FBS, Gibco) and 1% penicillin-streptomycin (Gibco). Non-adherent cells were removed after 72 h, and adherent cells were maintained at 37 °C in 5% CO_2 atmosphere. MSCs were passaged upon reaching 80% - 90% confluency and used at passages 3 - 5 for all experiments [23].

MSC characterization

MSCs were characterized by flow cytometry analysis of surface markers. Briefly, 1×10^5 cells were incubated with fluorochrome-conjugated antibodies against CD90-FITC, CD29-PE, CD45-APC, and CD31-PerCP (BD Biosciences, San Jose, CA, USA) for 30 min at 4 °C. Cells were washed, resuspended in PBS, and analyzed using BD FACSCanto II flow cytometer. Data analysis was performed using FlowJo software (BD Biosciences). Osteogenic differentiation was induced by culturing MSCs in osteogenic induction medium containing DMEM, 10% FBS, 10 mM β-glycerophosphate, 50 μM ascorbate-2-phosphate, and 100 nM dexamethasone (Sigma-Aldrich, St. Louis, MO, USA) for 21 days. Mineralization was assessed by Alizarin Red S staining. Adipogenic differentiation was performed using adipogenic induction medium containing DMEM, 10% FBS, 1 μM dexamethasone, 0.5 mM 3-isobutyl-1-methylxanthine, 10 μg/mL insulin, and 100 μM indomethacin (Sigma-Aldrich) for 14 days. Lipid accumulation was visualized by Oil Red O staining [24,25].

Paclitaxel conditioning protocol

MSCs at 70% - 80% confluence were treated with paclitaxel (Sigma-Aldrich) at concentrations of 10 and 20 μg/mL for 72 h. Following treatment, cells were washed extensively, and fresh medium was added for an additional 24 h to collect conditioned medium (CM-MSCs-Pax). The conditioned medium was centrifuged, filtered, and stored at −80 °C until use.

Assessment of MSC viability and proliferation

To evaluate the effect of paclitaxel on MSC viability, cells were exposed to 10 or 20 μg/mL paclitaxel for 72 h, and viability was assessed using the MTT assay according to the manufacturer's instructions. Briefly, MTT solution was added to each well and incubated for 4 h, after which the formazan crystals were dissolved in DMSO. Absorbance was measured at 570 nm using a microplate reader. Cell proliferation was also monitored by direct cell counting using trypan blue exclusion at the indicated time points. For the proliferation analysis, MSCs were seeded at a density of 1×10^4 cells per well in 12-well plates and treated with paclitaxel (10 or 20 μg/mL). Cell proliferation was evaluated at 0, 24, 48, 72, and 96 h by direct cell counting using trypan blue exclusion. The number of viable cells was recorded at each time point and used to generate proliferation curves.

Cytokine and growth factor analysis

The concentrations of IL-6, TGF-β1, VEGF, IL-10, and TNF-α in conditioned media were quantified using enzyme-linked immunosorbent assay (ELISA) kits according to the manufacturer's instructions (R&D Systems, Minneapolis, MN, USA). Briefly, 100 μL of conditioned medium samples were added to pre-coated 96-well plates and incubated for 2 h at room temperature. After washing, detection antibodies were added, followed by streptavidin-HRP conjugate. Color development was achieved using substrate solution, and absorbance was measured at 450 nm using a microplate reader (BioTek, Winooski, VT, USA) [26].

Animal ethics statement

All animal experiments were conducted in accordance with institutional guidelines and the ARRIVE 2.0 guidelines for the care and use of laboratory animals. The study protocol was reviewed and approved by the Animal Ethics Division of the Faculty of Medicine, Universitas Islam Sultan Agung Semarang (approval number: 264/VI/Komisi Bioetik/2025). All procedures involving animals were performed in compliance with relevant national and institutional regulations, and efforts were made to minimize animal suffering and reduce the number of animals used.

Animal Model and T cell isolation

Female BALB/c mice (6 - 8 weeks old) were used for tumor induction and T cell isolation. Mice were injected intraperitoneally with 1×10^6 4T1 breast cancer cells. Immune suppression was induced using dexamethasone (0.5 mg/kg) on the day of injection. After 21 days, tumor nodules were confirmed by histological analysis using hematoxylin-eosin staining and Ki67 immunofluorescence. Peripheral blood mononuclear cells were isolated and subjected to fluorescence-activated cell sorting (FACS). $CD8^+$ T cells were identified by sequential gating on lymphocytes (FSC/SSC), singlets, and $CD8^+CD4^-$ populations. Sorted cells were collected and cultured for 96 h prior to downstream experiments [27].

Human T cell isolation

Peripheral blood samples were collected from stage III breast cancer patients after written informed consent and approval from the institutional ethics committee (Ethics Committee approval number: 074/EC/KEPK/FKUA/2025). Peripheral blood mononuclear cells (PBMCs) were isolated by density-gradient centrifugation using Ficoll-Paque. Briefly, whole blood was diluted 1:1 with phosphate-buffered saline (PBS), layered over Ficoll-Paque, and centrifuged at 400 × g for 30 min at room temperature without brake. The PBMC layer was collected, washed twice with PBS, and resuspended in complete RPMI-1640 medium supplemented with 10% fetal bovine serum and 1% penicillin-streptomycin. T cells were isolated from PBMCs by fluorescence-activated cell sorting (FACS-based isolation). Cells were stained with anti-CD3, anti-CD4, and anti-CD8 antibodies, and viable $CD3^+$ T cells were gated for downstream experiments. Purified T cells were then cultured in conditioned medium from paclitaxel-conditioned MSCs (CM-MSCs-Pax) to induce activation. For comparison, control T cells were cultured with conditioned medium from untreated MSCs (CM-MSCs) or standard culture medium. Following activation, T cells were used for co-culture experiments with BCSCs.

T cell activation assay

Isolated $CD8^+$ T cells were treated with CM-MSCs-Pax for 24 and 48 h. T cell activation was assessed by measuring IL2RA (CD25) mRNA expression using quantitative reverse transcription-PCR (qRT-PCR). RNA extraction was performed using TRIzol reagent, followed by cDNA synthesis and real-time PCR using SYBR Green Master Mix. Expression levels were normalized to β-actin and calculated using the $2^{(-\Delta\Delta Ct)}$ method [28].

Co-culture cytotoxicity assays

BCSCs were co-cultured with activated T cells at T cell:BCSC ratios of 5:1 and 10:1 for 24, 48, and 72 h. To minimize bias in the MTT assay, non-adherent floating T cells were carefully removed before analysis. The adherent BCSCs were then washed 3 times with PBS to remove residual T cells. Cell viability was subsequently assessed using the MTT assay. Briefly, MTT solution (5 mg/mL) was added to each well and incubated for 4 h. The resulting formazan crystals were dissolved in DMSO, and absorbance was measured at 570 nm using a microplate reader.

Molecular Analysis

Total RNA was extracted from $CD8^+$ T cells or BCSCs after co-culture using a QIAGEN RNA isolation kit according to the manufacturer's instructions. RNA concentration and purity were determined spectrophotometrically, and RNA integrity was confirmed before downstream analysis. Complementary DNA (cDNA) was synthesized from 500ng of total RNA using a reverse transcription kit. Quantitative real-time PCR (qRT-PCR) was performed using SYBR Green Master Mix in a real-time PCR system. Gene-specific primers for mouse IL2RA, human caspase-3, human PD-L1 (CD274), and mouse/human β-actin were

used. Primer specificity was verified by melting-curve analysis and agarose gel electrophoresis of the PCR products. Relative gene expression was calculated using the $2^{-\Delta\Delta Ct}$ method and normalized to β-actin. All samples were analyzed in technical triplicate, and each experiment was repeated independently 3 times.

Table 1 Primer sequences.

Gene	Species	Forward primer (5'→3')	Reverse primer (5'→3')
Il2ra	Mouse	GCGTTGCTTAGGAAACTCCTGG	GCATAGACTGTGTTGGCTTCTGC
Caspase-3	Human	GGAAGCGAATCAATGGACTCTGG	GCATCGACATCTGTACCAGACC
PD-L1 (CD274)	Human	TGCCGACTACAAGCGAATTACTG	CTGCTTGTCCAGATGACTTCGG

Statistical analysis

All experiments were performed in triplicate with at least 3 independent biological replicates. Data are presented as mean ± standard deviation (SD). Statistical significance was determined using one-way ANOVA with post-hoc analysis. *p*-values < 0.05 were considered statistically significant.

Results and discussion

Successful isolation and characterization of CD44⁺/CD24⁻ BCSCs

The isolated BCSCs exhibited characteristic mesenchymal morphology with elongated, spindle-shaped cells arranged in parallel arrays with loose intercellular contacts (**Figure 1(A)**). MACS sorting of MDA-MB-231 cells successfully enriched the $CD44^+/CD24^-$ population to 80.7% purity (**Figures 1(B)** and **1(C)**). This morphology is consistent with the epithelial-to-mesenchymal transition (EMT) phenotype typically associated with increased invasive and migratory capabilities of cancer stem cells. Quantitative analysis of CD44 and CD24 expression confirmed the successful enrichment of the target population, with the majority of cells expressing high levels of CD44 and low or negative levels of CD24 (**Figure 1(C)**). This phenotype is well-established as a reliable marker for breast cancer stem cells and has been associated with enhanced tumorigenicity and therapeutic resistance.

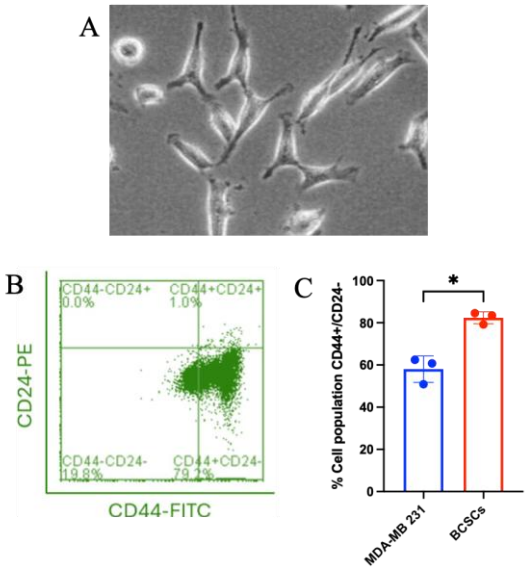


Figure 1 Characterization of breast cancer stem cells isolated from MDA-MB-231 cells. (A) Morphological analysis of BCSCs in 2D culture. Scale bar = 100 μm. (B) Flow cytometry analysis following MACS sorting showing enrichment of $CD44^+/CD24^-$ population. (C) Quantitative analysis of CD44 and CD24 expression levels in sorted BCSC population. T-test *p < 0.05 indicated a significant difference.

Characterization and validation of MSCs

MSCs demonstrated typical fibroblast-like morphology with elongated cell bodies and characteristic cytoplasmic projections (**Figure 2(A)**). Functional validation of MSC multipotency was confirmed through successful differentiation assays. Osteogenic differentiation resulted in the formation of mineralized nodules that stained positive with Alizarin Red S (**Figure 2(B)**), while adipogenic differentiation produced lipid-containing adipocytes positive for Oil Red O staining (**Figure 2(C)**). Flow cytometry analysis confirmed the mesenchymal phenotype, with high expression of CD90 (99.8%) and CD29 (97.7%), while showing minimal expression of hematopoietic marker CD45 (1.90%) and vascular marker CD31 (3.70%) (**Figure 2(D)**). These results confirm the successful isolation of bona fide MSCs suitable for subsequent conditioning experiments.

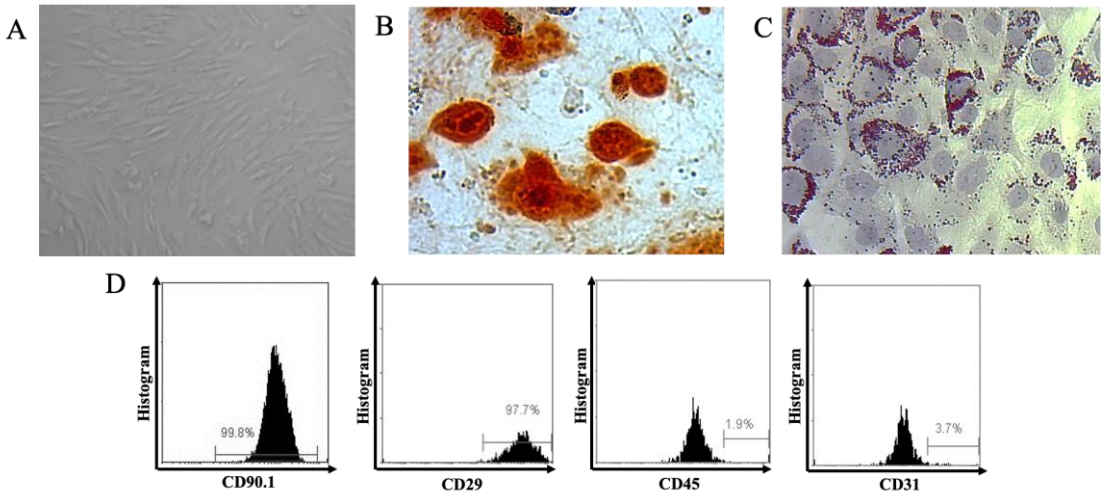


Figure 2 Characterization and validation of mesenchymal stem cells. (A) MSCs in 2D culture displaying typical fibroblast-like morphology with elongated cell bodies and cytoplasmic projections. Scale bar = 100 µm. (B) Osteogenic differentiation validation showing mineralized nodules stained with Alizarin Red S after 21 days of differentiation. Scale bar = 200 µm. (C) Adipogenic differentiation validation showing lipid droplet formation stained with Oil Red O after 14 days of differentiation. Scale bar = 200 µm. (D) Flow cytometry analysis of MSC surface markers.

Paclitaxel conditioning modifies MSC morphology and secretome

Treatment of MSCs with paclitaxel (10 and 20 µg/mL) for 72 h resulted in notable morphological changes, including reduced cell density and altered cell size while maintaining overall fibroblast-like morphology (**Figure 3(A)**). However, Cell viability as measured by the MTT assay showed no significant change after 72 h of treatment (**Figure 3(B)**). Furthermore, the proliferation rate was completely abated compared with controls (**Figure 3(C)**). These phenomena indicated that MSCs are relatively resistant to paclitaxel. Despite these morphological changes, the cells remained viable and metabolically active, as evidenced by their continued secretion of bioactive factors. ELISA analysis revealed significant alterations in the cytokine profile of conditioned medium from paclitaxel-treated MSCs. Notably, there were substantial increases in IL-6, TNF-α, and IL-10 levels compared to untreated controls (**Figures 3(D) - 3(F)**). IL-6 showed the most dramatic increase, which is particularly relevant given its role in T cell activation and maintenance of pro-inflammatory microenvironments. TNF-α elevation contributes to cytotoxicity against cancer cells, while IL-10 increase, despite being generally anti-inflammatory, may help prevent excessive inflammatory responses. In addition, paclitaxel-conditioned MSCs exhibited a marked alteration in their secretory profile, with significant decreases in VEGF and TGF-β levels compared with untreated controls (Figure 3G-H). The reduction in VEGF suggests a potential attenuation of angiogenic signaling, which may help limit tumor vascular support. In contrast, TGF-β was significantly reduced only at the

higher paclitaxel dose (20 μg/mL), indicating a dose-dependent suppressive effect on this immunosuppressive and pro-tumorigenic factor. In conjunction with increased levels of IL-6, TNF-α, and IL-10, these findings suggest that paclitaxel conditioning reprograms MSCs toward a more inflammatory, potentially anti-tumor secretome.

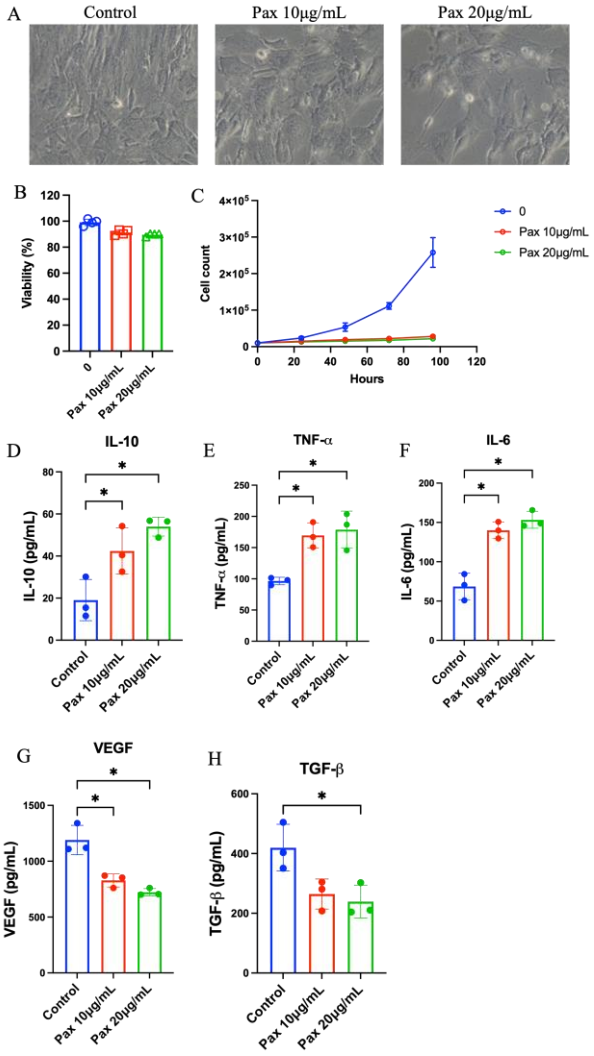


Figure 3 Paclitaxel conditioning of MSCs and secretome analysis. (A) Morphological comparison of MSCs following paclitaxel treatment (10 and 20 μg/mL) for 72 h. Scale bar = 100 μm. (B) MSCs viability was incubated with paclitaxel at 10 and 20 μg/mL for 72 h, and then treated with MTT. (C) Proliferation rate curves we've generated by counting MSCs treated with paclitaxel at 10 and 20 μg/mL for various lengths of time under trypan blue. (D-H) ELISA analysis of cytokine levels in conditioned medium of IL-6, TNF-α, and IL-10 following paclitaxel conditioning. Data presented as mean ± SD from 3 independent experiments. Statistical analysis performed using one-way ANOVA with Tukey's post-hoc test. *$p <$ 0.05 is significant compared to the control.

Successful tumor induction and T cell isolation

Intraperitoneal injection of 4T1 cells successfully induced tumor formation in BALB/c mice, with visible peritoneal nodules appearing 21 days post-injection (**Figure 4(A)**). Histological analysis using hematoxylin-eosin staining confirmed the presence of dense tumor cell populations with typical cancer morphology, including altered tissue architecture and immune cell infiltration (**Figure 4(B)**). Immunofluorescence staining for Ki67 demonstrated high proliferative activity within tumor nodules, with numerous cells showing positive nuclear staining (red signal) counterstained with DAPI (blue) (**Figure 4(C)**). This confirms the aggressive

growth characteristics of the induced tumors and validates the cancer model.

FACS sorting successfully isolated $CD8^+$ T cells from peripheral blood, comprising 13.60% of the total cell population (**Figure 4(D)**). Following 96-hour culture, the isolated T cells-maintained viability and formed characteristic T-lymphocyte cell clusters (**Figure 4(E)**).

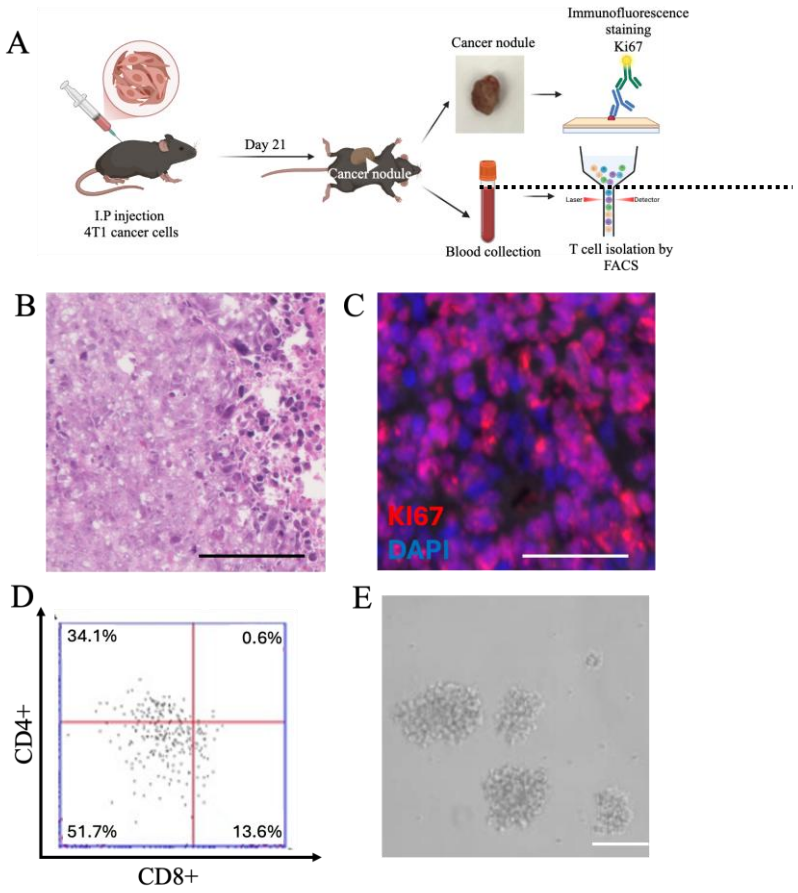


Figure 4 Tumor induction and T cell isolation from cancer-bearing mice. (A) Experimental scheme showing intraperitoneal injection of 4T1 cells (1×10^6) into BALB/c mice and subsequent T cell isolation by FACS. (B) Histological analysis of tumor nodules using hematoxylin-eosin staining shows dense tumor cell populations and altered tissue architecture. Scale bar = 100 μm. (C) Immunofluorescence staining for Ki67 (red) with DAPI counterstain (blue) demonstrating high proliferative activity in tumor nodules. Scale bar = 100 μm. (D) FACS analysis showing isolation of CD8+ T cells of peripheral blood cells. (E) Morphology of isolated CD8+ T cells after 96 h of culture showing viable cell clusters. Scale bar = 50 μm.

Enhanced T cell activation by paclitaxel-conditioned MSC medium

Treatment of $CD8^+$ T cells with CM-MSCs-Pax resulted in significant upregulation of IL2RA (CD25) mRNA expression, a well-established marker of T cell activation. Both 10 and 20 μg/mL paclitaxel-conditioned medium showed statistically significant increases in IL2RA expression compared to controls ($p < 0.01$) (**Figure 5**). Importantly, no significant difference was observed between 24-hour and 48-hour treatment durations, suggesting that maximal activation occurs within the first 24 h.

The upregulation of IL2RA is particularly significant as it encodes the CD25 subunit of the high-affinity IL-2 receptor, which is crucial for T cell proliferation and effector function. This finding demonstrates that paclitaxel conditioning creates a microenvironment conducive to T cell activation, likely by increasing the secretion of pro-inflammatory cytokines in the conditioned medium.

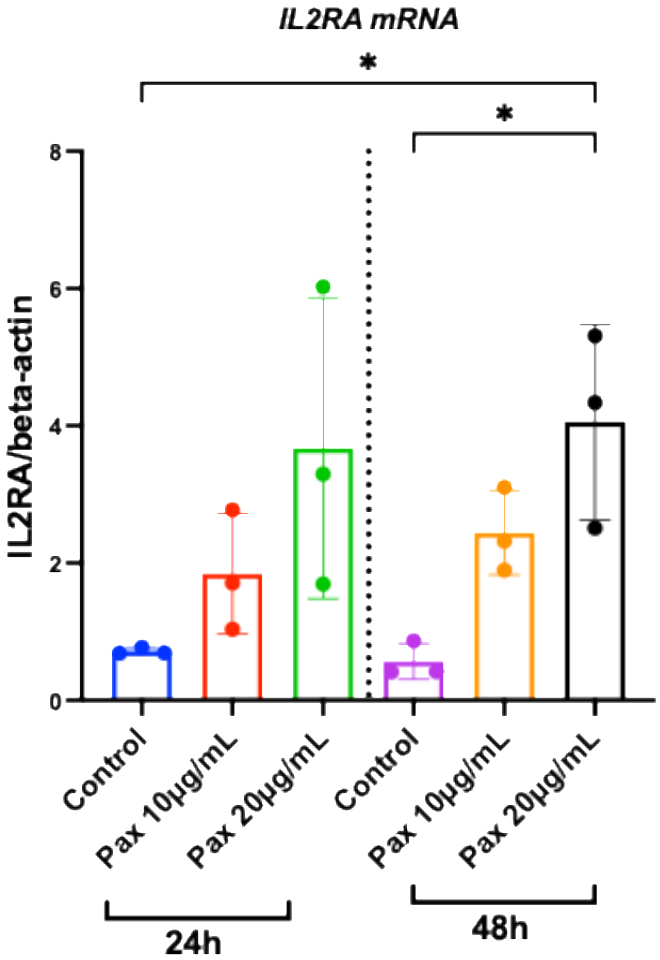


Figure 5 T cell activation analysis following treatment with paclitaxel-conditioned MSC medium. Quantitative RT-PCR analysis of IL2RA (CD25) mRNA expression normalized to β-actin at 24 and 48 h compared to controls. Data presented as mean ± SD from 3 independent experiments with technical triplicates. Statistical analysis performed using one-way ANOVA with Tukey's post-hoc test. *$p < 0.05$ is significant compared to the control.

Enhanced cytotoxicity against BCSCs

Co-culture experiments revealed dramatic differences in cytotoxicity between activated and unactivated T cells against BCSCs. Unactivated T cells reduced BCSC viability by only 30.20% after 72 h, while CM-MSCs-Pax-activated T cells at a 10:1 ratio achieved a remarkable 9.68% BCSC viability at the same time point (**Figure 6**). This represents a significant enhancement in cytotoxic efficiency, with activated T cells showing time-dependent increases in their anti-tumor effects. The dose-response relationship was evident, with 10:1 T cell:BCSC ratios showing superior cytotoxicity compared to 5:1 ratios. This suggests that adequate effector-to-target ratios are crucial for optimal therapeutic efficacy, consistent with clinical observations in adoptive T cell therapies.

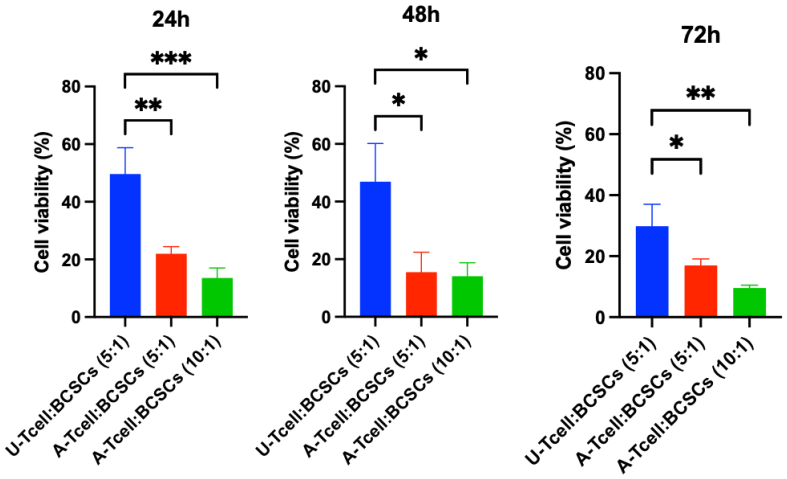


Figure 6 Cytotoxicity assay of activated T cells against breast cancer stem cells. MTT viability assay showing time-dependent reduction in BCSC viability following co-culture with activated T cells at 5:1 and 10:1 ratios, compared with unactivated T cell controls, at 24, 48, and 72 h. Data presented as mean ± SD from 3 independent experiments with 3 biological triplicates. Statistical analysis performed using one-way ANOVA with Tukey's post-hoc test. *$p < 0.05$. (U-Tcell: Unactivated T-cells, A-Tcell: Activated T-cells).

Validation in a human T cell-based co-culture system

To further address the possibility that the observed cytotoxicity in the mouse T cell–human BCSC system was influenced by xenogeneic reactivity, we performed an additional co-culture experiment using human T cells. Activated human T cells induced a pronounced decrease in BCSC viability and disruption of spheroid morphology compared with unactivated human T cells (**Figure 7(A)**). At 48 h, activated human T cells exhibited significantly higher cytotoxicity than unactivated human T cells (**Figure 7(B)**), even though the toxicity was lower in the mouse T cells in some ratios (**Figure 6**), this supporting the conclusion that the enhanced anti-BCSC effect is associated with T cell activation rather than species mismatch alone. These results strengthen the translational relevance of the CM-MSCs-Pax-induced immune activation strategy.

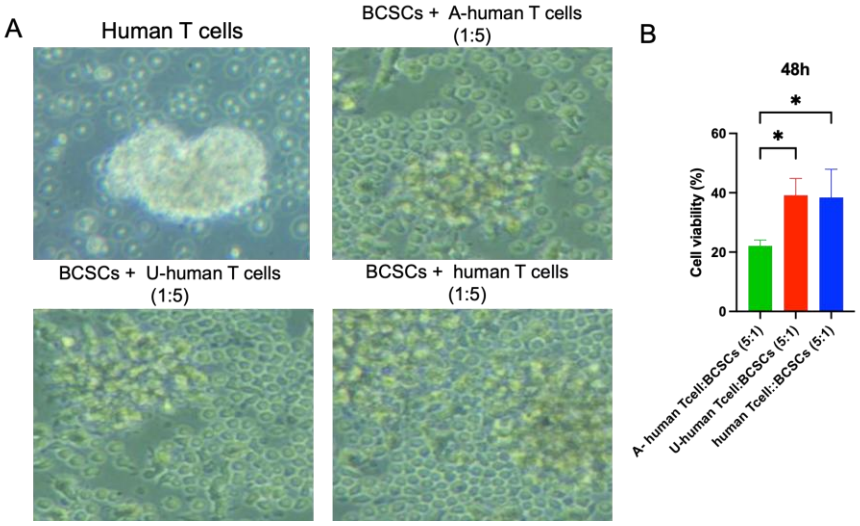


Figure 7 Validation of CM-MSCs-Pax-induced anti-BCSC cytotoxicity using human T cells. (A) Representative phase-contrast images showing BCSCs co-cultured with activated human T cells (A-human T cells), unactivated human T cells (U-human T cells), or human T cells only at an effector-to-target ratio of 1:5. (B) Quantification of BCSC viability at 48 h after co-culture. Data are presented as mean ± SD. Statistical analysis was performed using one-way ANOVA with Tukey's post hoc test. *$p < 0.05$.

Molecular mechanisms of enhanced cytotoxicity

Analysis of molecular markers revealed significant changes in both pro-apoptotic and immune checkpoint pathways. Caspase-3 expression, a key executioner of apoptosis, was significantly upregulated in BCSCs following co-culture with activated T cells compared to controls (**Figure 8(A)**). This increase in caspase-3 expression directly correlates with the observed reduction in cell viability and confirms that enhanced cytotoxicity occurs through apoptotic pathways.

PD-L1 expression was reduced in BCSCs following co-culture with activated T cells (**Figure 8(B)**). While this decrease may indicate modulation of immune checkpoint signaling, it may also reflect selective elimination of PD-L1-high BCSCs or a general reduction in viable tumor cell numbers [29]. Therefore, the observed reduction in PD-L1 should be interpreted cautiously, as it does not distinguish between active downregulation and changes in population composition.

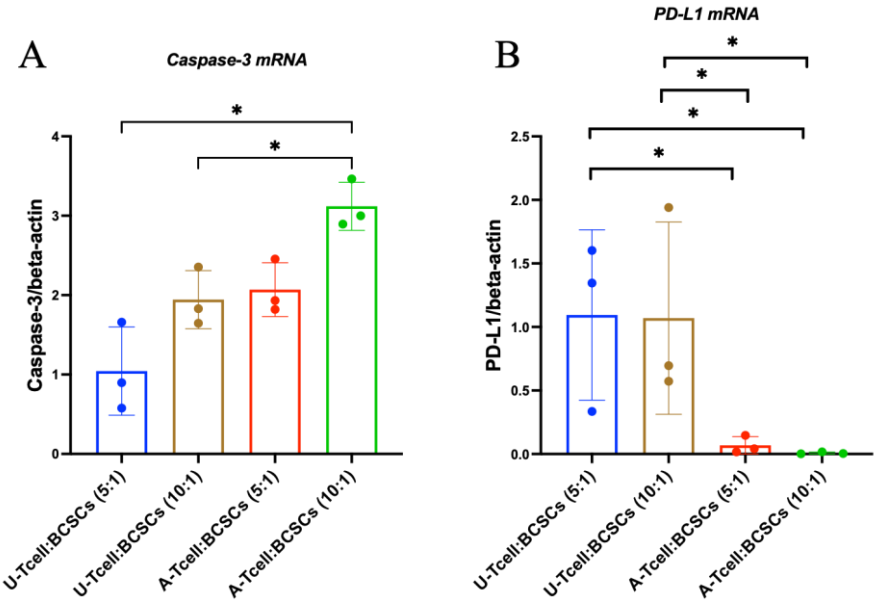


Figure 8 Molecular mechanism analysis of enhanced cytotoxicity. Quantitative RT-PCR analysis of (A) caspase-3 and (B) PD-L1 mRNA expression in BCSCs following co-culture with activated T cells. Data normalized to β-actin housekeeping gene and expressed as fold change relative to untreated control. Data presented as mean ± SD from 3 independent experiments with technical triplicates. Statistical analysis performed using one-way ANOVA with Tukey's post-hoc test. *$p < 0.05$. (U-Tcell: unactivated T-cells, A-Tcell: activated T-cells).

Our study presents a novel immunotherapeutic approach that combines the tumor-homing properties of MSCs with the cytotoxic potential of paclitaxel to enhance T cell-mediated immunity against breast cancer stem cells. The successful enrichment of $CD44^+/CD24^-$ BCSCs to 80.7% purity provides a robust model system for evaluating therapeutic interventions targeting this clinically relevant cell population. The morphological characteristics observed in our BCSC population, including the elongated spindle-shaped morphology and loose intercellular contacts, are consistent with previous reports describing the mesenchymal phenotype associated with cancer stem cells [9,30]. This phenotype reflects the epithelial-to-mesenchymal transition (EMT) program, which enhances cell motility and invasiveness, thereby contributing to the metastatic potential of these cells [31].

Conditioning MSCs with paclitaxel resulted in significant alterations in their secretory profile, creating a pro-inflammatory microenvironment that enhances immune cell activation. The observed increases in IL-6, TNF-α, and IL-10 reflect a complex cytokine milieu that collectively promotes anti-tumor immunity. IL-6 upregulation is particularly notable given its pleiotropic roles in cancer and immunity [32,33]. While IL-6 can support T cell activation, proliferation, and effector

differentiation, it is also well established that IL-6/STAT3 signaling contributes to tumor progression by maintaining cancer stem cell (CSC) properties, promoting survival, and enhancing chemoresistance [34,35]. In addition, IL-6-driven STAT3 activation has been shown to sustain stemness and tumor-initiating capacity, as well as resistance to chemotherapy [36]. Therefore, the increase in IL-6 observed in our system could, in principle, exert pro-tumorigenic effects. However, our findings suggest that the net outcome is skewed toward immune activation rather than tumor promotion. This may be explained by the concurrent elevation of strong pro-inflammatory mediators such as TNF-α, along with the presence of activated T cells, which together create a dominant cytotoxic environment that overrides potential IL-6-mediated tumor-supportive signaling [33,37]. In addition, the co-culture system directly exposes BCSCs to immune effector cells, limiting the opportunity for IL-6/STAT3 signaling to drive long-term stemness or resistance programs. It is also possible that IL-6 primarily acts on T cells, enhancing their activation and persistence rather than promoting BCSC survival.

The elevation of TNF-α in conditioned medium is consistent with the pro-inflammatory shift induced by paclitaxel treatment. TNF-α not only enhances T cell activation but also exerts direct cytotoxic effects on cancer cells via death receptor pathways [38,39]. This dual mechanism likely contributes to the enhanced anti-tumor effects observed in our co-culture experiments. Notably, IL-10 levels were also elevated following paclitaxel conditioning. IL-10 is widely recognized for its immunosuppressive functions, including inhibition of T cell effector activity, reduction of antigen presentation, and promotion of T cell exhaustion in chronic inflammatory or tumor settings [25,40]. Emerging evidence indicates that IL-10 can also support $CD8^+$ T cell survival, limit activation-induced cell death, and preserve functional capacity under sustained stimulation, particularly when co-existing with strong pro-inflammatory cues [41]. In our system, the simultaneous upregulation of TNF-α and IL-6 likely counterbalances the suppressive effects of IL-10, maintaining an overall activation-permissive environment. Rather than inducing functional exhaustion, IL-10 may act as a regulatory checkpoint to prevent excessive inflammatory damage while allowing sustained T cell activity. This interpretation is consistent with reports demonstrating that IL-10 can enhance cytotoxic T cell responses and improve anti-tumor immunity under specific conditions, particularly in combination with pro-inflammatory signaling [42]. Together, these findings suggest that paclitaxel conditioning establishes a finely tuned cytokine milieu in which dominant pro-inflammatory signals drive T cell activation, while IL-10 provides regulatory control to sustain viability and prevent overstimulation. This balanced immune modulation may be critical for achieving effective and durable anti-tumor responses.

The significant upregulation of IL2RA (CD25) expression following treatment with CM-MSCs-Pax provides clear evidence of enhanced T cell activation. CD25 forms part of the high-affinity IL-2 receptor complex and its upregulation is one of the earliest and most reliable markers of T cell activation. The rapid kinetics of this response, with maximal activation achieved within 24 h, suggests that the conditioning medium contains potent T cell stimulatory factors. Our findings are consistent with recent studies demonstrating that chemotherapy-conditioned MSCs can enhance immune responses against cancer cells. A study reported similar findings using doxorubicin-conditioned MSCs, showing enhanced natural killer cell activation [43,44]. However, our study is the first to demonstrate this approach specifically targeting $CD44^+/CD24^-$ breast cancer stem cells using paclitaxel conditioning. The choice of paclitaxel for MSC conditioning is strategically important, as this agent has well-documented immunomodulatory effects beyond its cytotoxic properties. Paclitaxel can activate toll-like receptor 4 (TLR4) signaling pathways, leading to dendritic cell maturation and enhanced antigen presentation [45-47]. These properties likely contribute to the observed enhancement in T cell activation when MSCs are conditioned with this agent.

In addition, the dramatic reduction in BCSC viability achieved by CM-MSCs-Pax-activated T cells represents a significant therapeutic advance. The ability to reduce BCSC viability to less than 10% using a 10:1 effector-to-target ratio suggests potential clinical applicability, as these ratios are achievable through adoptive T cell transfer protocols. The time-dependent increase in cytotoxicity, with maximal effects observed at 72 h, provides important insights into the kinetics of

T cell-mediated killing. This prolonged cytotoxic activity suggests that activated T cells maintain their effector function for extended periods, which is crucial for clinical efficacy, where sustained anti-tumor responses are required. Comparison with existing immunotherapeutic approaches highlights the potential advantages of our strategy. Traditional checkpoint inhibitor therapies have shown limited efficacy against breast cancer, particularly triple-negative breast cancer where BCSCs are prevalent [47]. CAR-T cell therapies, while promising, face significant challenges in solid tumors due to antigen heterogeneity and the immunosuppressive microenvironment [48]. Our approach addresses these limitations by using broadly activated T cells that can recognize multiple tumor antigens and by creating a pro-inflammatory microenvironment that counteracts immunosuppression.

The molecular analysis revealed 2 key features associated with enhanced cytotoxicity including increased apoptotic signaling, as indicated by caspase-3 upregulation, and a reduction in PD-L1 expression. Caspase-3 activation confirms that cell death occurs predominantly through apoptotic pathways, which is advantageous given its controlled and non-inflammatory nature [49]. The strong correlation between caspase-3 expression and reduced cell viability suggests that T cell-mediated cytotoxicity effectively engages programmed cell death mechanisms in BCSCs. The observed decrease in PD-L1 expression is notable; however, its interpretation requires caution. While this may suggest reduced immune evasion capacity, an alternative explanation is that activated T cells preferentially eliminate PD-L1-high BCSCs, leading to an apparent reduction in overall PD-L1 levels [49]. Additionally, decreased PD-L1 expression may simply reflect reduced numbers of viable tumor cells following cytotoxicity rather than active checkpoint regulation [29]. Therefore, the current data do not definitively distinguish between true PD-L1 downregulation and shifts in tumor cell population dynamics. To clarify this mechanism, further analysis is required including flow cytometric assessment of PD-L1 expression gated specifically on viable BCSCs would help determine whether PD-L1 is actively downregulated at the single-cell level. Complementary approaches such as longitudinal tracking of PD-L1 expression or normalization to viable cell counts would also strengthen mechanistic conclusions. Despite this limitation, the combined increase in apoptotic signaling and reduction in overall PD-L1-associated tumor burden suggest that activated T cells effectively target both the survival and immune evasion characteristics of BCSCs [50,51]. This dual effect, whether driven by direct regulation or selective elimination, supports the therapeutic potential of this approach while highlighting the need for more refined mechanistic studies.

Our approach offers several advantages over existing immunotherapeutic strategies for breast cancer. Compared to checkpoint inhibitors such as pembrolizumab, which have shown limited efficacy in breast cancer [20,52], our method directly enhances T cell activation rather than merely removing inhibitory signals. This approach may be particularly beneficial in "cold" tumors with limited T cell infiltration, as it provides both activated effector cells and a pro-inflammatory microenvironment. Compared with CAR-T cell therapies, our approach avoids the limitations of single-antigen targeting. BCSCs exhibit phenotypic plasticity and antigen heterogeneity, rendering single-target approaches potentially vulnerable to escape mechanisms. By using polyclonally activated T cells, our strategy can simultaneously recognize multiple tumor-associated antigens, reducing the likelihood of immune escape. The use of autologous MSCs as vehicles for immune enhancement also offers practical advantages. MSCs can be easily isolated from patients, expanded ex vivo, and conditioned with paclitaxel before reinfusion. This approach avoids the complex genetic modifications required for CAR-T cells while maintaining the potential for personalized therapy.

While our results are promising, several limitations should be acknowledged. Our study was conducted entirely in vitro using the MDA-MB-231 cell line, which may not fully represent primary BCSC behavior, future studies should incorporate patient-derived BCSCs. The mouse model for T cell isolation may not fully recapitulate human immune responses, necessitating validation in human T cells and humanized mouse models. In addition, Optimal paclitaxel concentration and conditioning duration (72 h) require further dose-response optimization. On the other hand, stem cell identity was primarily confirmed by $CD44^{+}/CD24^{-}$ surface markers and morphology, rather

than by functional assays such as mammosphere formation or ALDH activity. Future work should also include *in vivo* validation using orthotopic breast cancer models, long-term assessment of T cell persistence and resistance mechanisms, proteomic analysis of secreted factors to identify additional bioactive factors, and combination approaches with immunomodulatory agents or checkpoint inhibitors to enhance therapeutic efficacy.

Conclusions

This study demonstrates that paclitaxel conditioning of mesenchymal stem cells creates a pro-inflammatory microenvironment that significantly enhances T cell activation and cytotoxicity against $CD44^+/CD24^-$ breast cancer stem cells. The approach achieved remarkable therapeutic efficacy, reducing BCSC viability to less than 10% through dual mechanisms involving enhanced apoptotic signaling and reduced immune evasion. This novel immunotherapeutic approach represents a promising strategy for targeting therapy-resistant breast cancer stem cell populations and warrants further investigation for clinical translation. The combination of established clinical procedures and demonstrated efficacy against cancer stem cells positions this approach as a potential breakthrough in breast cancer immunotherapy.

Acknowledgements

We thank the patients who participated in this study and provided blood samples. We acknowledge the technical support provided by the Flow Cytometry Core Facility and Cell Culture Laboratory. This research was funded by the Fundamental Research Scheme of the Directorate of Research, Technology, and Community Service (DRTPM), Ministry of Education, Culture, Research, and Technology of the Republic of Indonesia, in 2025, under Grant No. 33/UN5.4.10.K/PT.01.03/KP-DPPM/2025.

Declaration of generative AI in scientific writing

The author utilized artificial intelligence tools solely for grammar and language editing purposes to enhance readability, as the author is not a native English speaker. The AI was not used for data analysis, interpretation, or content generation. The author takes full responsibility for the accuracy, integrity, and originality of all content presented in the manuscript.

CRediT author statement

Dedy Hermansyah: Conceptualization, Methodology, Supervision, Validation, Project administration, Funding acquisition, and Writing - Reviewing and Editing. **Siti Syarifah:** Investigation, Data curation, Formal analysis, Validation, Visualization, and Writing–original draft. **Adi Muradi Muhar:** Conceptualization, Methodology, Resources, Supervision, Validation, and Writing–review & editing. **Nur Dina Amalina:** Investigation, Data curation, Formal analysis, Validation, Visualization, and Writing–original draft.

References

[1] SM Lima, RD Kehm and MB Terry. Global breast cancer incidence and mortality trends by region, age-groups, and fertility patterns. *eClinicalMedicine* 2021; **38**, 100985.

[2] H Zeng and G Lu. Research progress of breast cancer stem cell stemness and breast cancer recurrence. *Journal of Biosciences and Medicines* 2024; **12(8)**, 281-294.

[3] Y Feng, M Spezia, S Huang, C Yuan, Z Zeng, L Zhang, X Ji, W Liu, B Huang, W Luo, B Liu, Y Lei, S Du, A Vuppalapati, HH Luu, RC Haydon, TC He and G Ren. Breast cancer development and progression: Risk factors, cancer stem cells, signaling pathways, genomics, and molecular pathogenesis. *Genes & Diseases* 2018; **5(2)**, 77-106.

[4] W Shuo, Z Ying, C Weihong, L Jie, Z Yuren, F Huiting, X Yonggang, L Hongsheng and HS Lin. Breast cancer stem-like cells can promote metastasis by activating platelets and down-regulating antitumor activity of natural killer cells. *Journal of Traditional Chinese Medicine* 2016; **36(4)**, 530-537.

[5] JS Crabtree and L Miele. Breast cancer stem cells. *Biomedicines* 2018; **6(3)**, 77.

[6] D Hermansyah, S Syarifah, AM Muhar and A Putra. Unveiling paclitaxel-induced mesenchymal stem cells: Orchestrating *Nrf2* modulation and apoptosis in $CD44^+/CD24^-$ cancer stem cells.

Breast Cancer: Targets and Therapy 2024; **16**, 319-328.

[7] MA Elbaiomy, T Akl, N Atwan, AA Elsayed, M Elzaafarany and S Shamaa. Clinical impact of breast cancer stem cells in metastatic breast cancer patients. *Journal of Oncology* 2020; **2020**, 2561726.

[8] WC Sin and CL Lim. Breast cancer stem cells—from origins to targeted therapy. *Stem Cell Investigation* 2017; **4**, 96.

[9] LV Nalla, K Kalia and A Khairnar. Self-renewal signaling pathways in breast cancer stem cells. *The International Journal of Biochemistry & Cell Biology* 2019; **107**, 140-153.

[10] P Darvin, VS Nair and E Elkord. PD-L1 expression in human breast cancer stem cells is epigenetically regulated through posttranslational histone modifications. *Journal of Oncology* 2019; **2019**, 3958908.

[11] S Almozyan, D Colak, F Mansour, A Alaiya, O Al-Harazi, A Qattan, F Al-Mohanna, M Al-Alwan and H Ghebeh. PD-L1 promotes OCT4 and Nanog expression in breast cancer stem cells by sustaining PI3K/AKT pathway activation. *International Journal of Cancer* 2017; **141(7)**, 1402-1412.

[12] J Chu, Y Li, X Fan, J Ma, J Li, G Lu, Y Zhang, Y Huang, W Li, X Huang, Z Fu, Y Yin and H Yuan. MiR-4319 suppress the malignancy of triple-negative breast cancer by regulating self-renewal and tumorigenesis of stem cells. *Cellular Physiology and Biochemistry* 2018; **48(2)**, 593-604.

[13] T Li, C Zhang, Y Ding, W Zhai, K Liu, F Bu, T Tu, L Sun, W Zhu, F Zhou, W Qi, J Hu, H Chen and X Sun. Umbilical cord-derived mesenchymal stem cells promote proliferation and migration in MCF-7 and MDA-MB-231 breast cancer cells through activation of the ERK pathway. *Oncology Reports* 2015; **34(3)**, 1469-1477.

[14] M Szewc, E Radzikowska-Bűchner, P Wdowiak, J Kozak, P Kuszta, E Niezabitowska, J Matysiak, K Kubiński and M Masłyk. MSCs as tumor-specific vectors for the delivery of anticancer agents—a potential therapeutic strategy in cancer diseases: Perspectives for quinazoline derivatives. *International Journal of Molecular Sciences* 2022; **23(5)**, 2745.

[15] R Hass. Role of msc in the tumor microenvironment. *Cancers* 2020; **12(8)**, 2107.

[16] HM Nawara, SM Afify, G Hassan, MH Zahra, A Seno and M Seno. Paclitaxel-based chemotherapy targeting cancer stem cells from mono- to combination therapy. *Biomedicines* 2021; **9(5)**, 500.

[17] RC Sterner and RM Sterner. CAR-T cell therapy: Current limitations and potential strategies. *Blood Cancer Journal* 2021; **11(4)**, 69.

[18] C D'Accardo, G Porcelli, LR Mangiapane, C Modica, VD Pantina, N Roozafzay, S Di Franco, M Gaggianesi, V Veschi, M Lo Iacono, M Todaro, A Turdo and G Stassi. Cancer cell targeting by CAR-T cells: A matter of stemness. *Frontiers in Molecular Medicine* 2022; **2**, 1055028.

[19] HE Marei, K Bedair, A Hasan, L Al-Mansoori, S Caratelli, G Sconocchia, A Gaiba and C Cenciarelli. Current status and innovative developments of CAR-T-cell therapy for the treatment of breast cancer. *Cancer Cell International* 2025; **25(1)**, 3.

[20] H Wang, G Kaur, AI Sankin, F Chen, F Guan and X Zang. Immune checkpoint blockade and CAR-T cell therapy in hematologic malignancies. *Journal of Hematology & Oncology* 2019; **12(1)**, 59.

[21] M Suzery, B Cahyono and ND Amalina. *Citrus sinensis* (L) peels extract inhibits metastasis of breast cancer cells by targeting the downregulation matrix metalloproteinases-9. *Open Access Macedonian Journal of Medical Sciences* 2021; **9(B)**, 464-469.

[22] M Suzery, B Cahyono and ND Amalina. Antiproliferative and apoptosis effect of hyptolide from *Hyptis pectinata* (L.) Poit on human breast cancer cells. *Journal of Applied Pharmaceutical Science* 2020; **10(2)**, 001-006.

[23] M Fredianto, H Herman, YD Ismiarto, A Putra, I Alif, ND Amalina and MA Nazar. Secretome of hypoxia-preconditioned mesenchymal stem cells enhance the expression of HIF-1a and bFGF in a rotator cuff tear model. *Medicinski Glasnik* 2023; **20(2)**, 242-248.

[24] AM Muhar, F Makharim, D Hermansyah, A Putra, N Hidayah, ND Amalina and I Alif. Hypoxic mesenchymal stem cell-conditioned medium accelerates wound healing by regulating IL-10 and TGF-β levels in a full-thickness-wound rat model. *Indonesian Journal of Biotechnology* 2022; **27(4)**, 187-194.

[25] YW Prajoko, A Putra, BT Dirja, AM Muhar and ND Amalina. The ameliorating effects of MSCs in controlling Treg-mediated B-cell depletion by indoleamine 2, 3-dioxygenase induction in PBMC of SLE patients. *Open Access Macedonian Journal of Medical Sciences* 2022; **10(A)**, 6-11.

[26] BT Dirja, EH Wardoyo, A Putra and ND Amalina. Enhanced third degree burn wound healing by hypoxic mesenchymal stem cells' secretome: IL-10 upregulation and TNF-α/PGE2 suppression. *Trends in Sciences* 2024; **21(10)**, 8288.

[27] A Chaudhry, RM Samstein, P Treuting, Y Liang, MC Pils, JM Heinrich, RS Jack, FT Wunderlich, JC Brüning, W Müller and AY Rudensky. Interleukin-10 signaling in regulatory T cells is required for suppression of Th17 cell-mediated inflammation. *Immunity* 2011; **34(4)**, 566-578.

[28] DA Paramita, D Hermansyah and ND Amalina. Regulation of p53 and *survivin* by *Curcuma longa* extract to *caspase-3* dependent apoptosis in triple negative breast cancer cells. *Medicinski Glasnik* 2022; **19(2)**, 189-196.

[29] Q Tang, Y Chen, X Li, S Long, Y Shi, Y Yu, W Wu, L Han and S Wang. The role of PD-1/PD-L1 and application of immune-checkpoint inhibitors in human cancers. *Frontiers in Immunology* 2022; **13**, 964442.

[30] MG Scioli, G Storti, F D'Amico, P Gentile, G Fabbri, V Cervelli and A Orlandi. The role of breast cancer stem cells as a prognostic marker and a target to improve the efficacy of breast cancer therapy. *Cancers* 2019; **11(7)**, 1021.

[31] H Xu, Y Zhou, W Li, B Zhang, H Zhang, S Zhao, P Zheng, H Wu and J Yang. Tumor-derived mesenchymal-stem-cell-secreted IL-6 enhances resistance to cisplatin via the STAT3 pathway in breast cancer. *Oncology Letters* 2018; **15(6)**, 9142-9150.

[32] DE Johnson, RA O'Keefe and JR Grandis. Targeting the IL-6/JAK/STAT3 signalling axis in cancer. *Nature Reviews Clinical Oncology* 2018; **15(4)**, 234-248.

[33] T Hirano. IL-6 in inflammation, autoimmunity and cancer. *International Immunology* 2021; **33(3)**, 127-148.

[34] H Jeong, J Koh, S Kim, J Yim, SG Song, H Kim, Y Li, SH Lee, YK Chung, H Kim, CH Lee, HY Kim, B Keam, SH Lee, DH Chung and YK Jeon. Cell-intrinsic PD-L1 signaling drives immunosuppression by myeloid-derived suppressor cells through IL-6/Jak/Stat3 in PD-L1-high lung cancer. *Journal for ImmunoTherapy of Cancer* 2025; **13(3)**, e010612.

[35] SA Nish, D Schenten, T Wunderlich, SD Pope, Y Gao, N Hoshi, S Yu, X Yan, HK Lee, L Pasman, I Brodsky, B Yordy, H Zhao, J Bruning and R Medzhitov. T cell-intrinsic role of IL-6 signaling in primary and memory responses. *eLife* 2014; **3**, e01949.

[36] B Huang, X Lang and X Li. The role of IL-6/JAK2/STAT3 signaling pathway in cancers. *Frontiers in Oncology* 2022; **12**, 1023177.

[37] Y Wang, AHH Van Boxel-Dezaire, H Cheon, J Yang and GR Stark. STAT3 activation in response to IL-6 is prolonged by the binding of IL-6 receptor to EGF receptor. *Proceedings of the National Academy of Sciences of the United States of America* 2013; **110(42)**, 16975-16980.

[38] FK Hartati, SB Widjanarko, TD Widyaningsih and M Rifa'i. Anti-inflammatory evaluation of black rice extract inhibits TNF-α, IFN-γ and IL-6 cytokines produced by immunocompetent cells. *Food and Agricultural Immunology* 2017; **28(6)**, 1116-1125.

[39] A Putra, FB Ridwan, AI Putridewi, AR Kustiyah, K Wirastuti, NAC Sadyah, I Rosdiana and D Munir. The role of TNF-α induced MSCs on suppressive inflammation by increasing TGF-β and IL-10. *Open Access Macedonian Journal of Medical Sciences* 2018; **6(10)**, 1779-1783.

[40] DM Darlan, D Munir, A Putra, I Alif, ND Amalina, NK Jusuf and IB Putra. Revealing the decrease of indoleamine 2,3-dioxygenase as a major constituent for B cells survival post-mesenchymal stem cells co-cultured with peripheral blood mononuclear cell (PBMC) of

systemic lupus erythematosus (SLE) patients. *Medicinski Glasnik* 2022; **19(1)**, 12-18.

[41] J Xi, M Xu, Z Song, H Li, S Xu, C Wang, H Song and J Bai. Stimulatory role of interleukin 10 in CD8+ T cells through STATs in gastric cancer. *Tumor Biology* 2017; **39(5)**, 1010428317706209.

[42] Z Guo, Q He, Y Zhang, Y Li and Z Zhang. Mechanisms of interleukin-10-mediated immunosuppression in viral infections. *Pathogens* 2025; **14(10)**, 989.

[43] G Wang, D Zhang, S Yang, Y Wang, Z Tang and X Fu. Co-administration of genistein with doxorubicin-loaded polypeptide nanoparticles weakens the metastasis of malignant prostate cancer by amplifying oxidative damage. *Biomaterials Science* 2018; **6(4)**, 827-835.

[44] ND Amalina, IP Nurhayati and E Meiyanto. Doxorubicin induces lamellipodia formation and cell migration. *Indonesian Journal of Cancer Chemoprevention* 2017; **8(2)**, 61-67.

[45] S Ran. The role of TLR4 in chemotherapy-driven metastasis. *Cancer Research* 2015; **75(12)**, 2405-2410.

[46] J Abdi, I Rashedi and A Keating. Concise review: TLR pathway-miRNA interplay in mesenchymal stromal cells: Regulatory roles and therapeutic directions. *Stem Cells* 2018; **36(11)**, 1655-1662.

[47] LW Pfannenstiel, SS Lam, LA Emens, EM Jaffee and TD Armstrong. Paclitaxel enhances early dendritic cell maturation and function through TLR4 signaling in mice. *Cellular Immunology* 2010; **263(1)**, 79-87.

[48] MA Huseni, L Wang, JE Klementowicz, K Yuen, B Breart, C Orr, LF Liu, Y Li, V Gupta, C Li, D Rishipathak, J Peng, Y Şenbabaoğlu, Z Modrusan, S Keerthivasan, S Madireddi, YJ Chen, EJ Fraser, N Leng, H Hamidi, H Koeppen, J Ziai, K Hashimoto, M Fassò, P Williams, DF McDermott, JE Rosenberg, T Powles, LA Emens, PS Hegde, I Mellman, SJ Turley, MS Wilson, S Mariathasan, L Molinero, M Merchant and NR West. CD8+ T cell-intrinsic IL-6 signaling promotes resistance to anti-PD-L1 immunotherapy. *Cell Reports Medicine* 2023; **4(1)**, 100878.

[49] X Pu, SJ Storr, Y Zhang, EA Rakha, AR Green, IO Ellis and SG Martin. Caspase-3 and caspase-8 expression in breast cancer: Caspase-3 is associated with survival. *Apoptosis* 2017; **22(3)**, 357-368.

[50] KM Zak, P Grudnik, K Magiera, A Dömling, G Dubin and TA Holak. Structural biology of the immune checkpoint receptor PD-1 and its ligands PD-L1/PD-L2. *Structure* 2017; **25(8)**, 1163-1174.

[51] M Elfoly, JY Mirza, A Alaiya, AA Al-Hazzani, A Tulbah, M Al-Alwan and H Ghebeh. PD-L1 intrinsically promotes the proliferation of breast cancer cells through the SKP2-p27/p21 axis. *Cancer Cell International* 2024; **24(1)**, 161.

[52] M Jin, J Fang, J Peng, X Wang, P Xing, K Jia, J Hu, D Wang, Y Ding, X Wang, W Li and Z Chen. PD-1/PD-L1 immune checkpoint blockade in breast cancer: Research insights and sensitization strategies. *Molecular Cancer* 2024; **23(1)**, 266.